

Dynamical and Stereochemical Aspects of Photodissociation

RICHARD N. DIXON

School of Chemistry, University of Bristol, Cantock's Close, Bristol BS8 1TS, U.K.

Received July 9, 1990 (Revised Manuscript Received October 9, 1990)

I. Introduction

The activation of chemical reactions by light is essential to life and also plays a role in many other processes of importance to mankind. The range of reaction times is huge. Fortunately the fading of dyes may take years or even centuries, whereas the imprinting of a latent image in our cameras is sufficiently instantaneous that we can use it to "freeze" motion too fast for our unaided senses. The understanding of the factors that control photochemical reactions increased dramatically with the invention by Norrish and Porter of the techniques of flash photolysis and kinetic spectroscopy.¹ These made it possible to freeze, and thus chart, the evolution of the reaction on its path from activated reactant to products.

The early experiments of this type used flash lamps, giving a range of activation energies. They also used absorption spectrometry, which necessitated high pressure gas samples or fairly concentrated solutions, with the result that the product molecules rapidly thermalized their energy distribution. While such experiments often led to the identification of the reaction pathways and the detection of unstable intermediates, they did not necessarily reveal the detailed motion during the primary bond-breaking step. This limitation has now been removed by the use of lasers, and particularly tunable dye lasers, both to initiate photochemical decomposition and to probe the identity of, and energy disposal within, the primary reaction products. These advances are a consequence of four properties of lasers: monochromaticity, which often permits parent molecule activation and product detection at a quantum-specific level; intensity, which enhances the sensitivity of product detection, permitting low enough pressures in the gas phase to avoid collisional relaxation; directionality and polarization, which can be used to probe the correlation between vectorial properties of the reactant and product motions, thereby giving insight into the stereospecificity of the primary reaction step; and pulse duration, which at its shortest can match the femtosecond time scale of the motions of the atoms in a molecule.

Photochemical activation usually involves electronic excitation, in which the parent molecule is promoted

from motion on the ground-state potential surface to an excited surface. These excited states may be grouped into two broad classes according to their stability to nuclear motion. *Direct dissociation* on a potential surface repulsive between two parts of the molecule occurs on the time scale of a vibrational period (~ 30 fs) and is characterized by a structureless absorption spectrum for the parent molecule (recall the uncertainty principle). In contrast, a highly structured absorption spectrum indicates the presence of a potential well in the excited-state surface, giving rise to long-lived states which may be characterized by excited-state quantum numbers. Any dissociation from these states occurs on a slower time scale than direct dissociation and is termed *predissociation*. Its occurrence may be recognized (i) via line broadening in the absorption spectrum, (ii) by weakening or breaking off in the parent emission spectrum, or (iii) by the detection of photofragments or reaction products.

In a diatomic molecule the (one) vibrational coordinate is also the reaction coordinate for dissociation (Figure 1). Predissociation of a long-lived state can only occur by quantum tunneling through a barrier or by a change of electronic state near a curve crossing. On dissociation any excess energy above the electronic energy of the separated atoms (the *available energy*) must appear in their mutual recoil:

$$E_{\text{parent}} + h\nu - E_{\text{atoms}} \equiv E_{\text{available}} \rightarrow E_{\text{recoil}} \quad (1)$$

Polyatomic molecules have a much richer diversity of dissociation mechanisms, since energy can flow between many internal modes of excitation, and the distinction between direct and indirect dissociation is less clear-cut than in diatomic molecules. In his classic book, Herzberg² classified polyatomic predissociation mechanisms into case I, *predissociation by electronic transition*; case II, *predissociation by vibration*; and case III, *predissociation by rotation*. It is now recognized that it is possible for these processes to occur simultaneously with rates that may vary with the vibrational or rotational quantum numbers, giving a quantum-state specificity to the mechanism. An extreme form of this is known for SiH_2^+ , where predissociation occurs competitively into the two chemically distinct channels $\text{Si}^+ + \text{H}_2$ and $\text{SiH}^+ + \text{H}$ with the branching ratio³ showing marked rotational dependence.

Energy flow between internal modes during dissociation is not limited to long-lived states. In direct dissociation of a polyatomic molecule AB, the potential will be repulsive along the coordinate R_{AB} between the centers of mass of the fragments A and B, thereby

(1) Porter, G. *Proc. R. Soc.* **1950**, *A200*, 284.

(2) Herzberg, G. *Molecular Spectra and Molecular Structure III. Electronic Spectra and Electronic Structure of Polyatomic Molecules*; Van Nostrand: Princeton, 1966.

(3) Curtis, M. C.; Jackson, P. A.; Sarre, P. J.; Whitham, C. J. *Mol. Phys.* **1985**, *56*, 485.

Richard N. Dixon was born in Borough Green, Kent, England, on Dec 25, 1930, and is now the Alfred Capper Pass Professor of Chemistry and a Pro-Vice-Chancellor at the University of Bristol. He received his B.Sc. degree (1951) from London University and Ph.D. (1955) and Sc.D. (1976) degrees from Cambridge University. After a spell with the UKAEA, he was a post-doctoral fellow in Canada at the University of Western Ontario (1956-1957) and the National Research Council (1957-1959). He returned to England to the University of Sheffield in 1959 and was appointed Professor at Bristol in 1969. He was an ICI Fellow (1959-1960) and the Sorby Research Fellow of the Royal Society (1964-1969) and was elected FRS in 1986. He won the Corday-Morgan medal of the Royal Society of Chemistry for 1966 and their medal for spectroscopy in 1984. His research centers on molecular spectroscopy, photochemistry, energy transfer, and molecular quantum dynamics. He currently serves on the editorial boards of four journals and is Vice-President of the Faraday Division of the Royal Society of Chemistry.

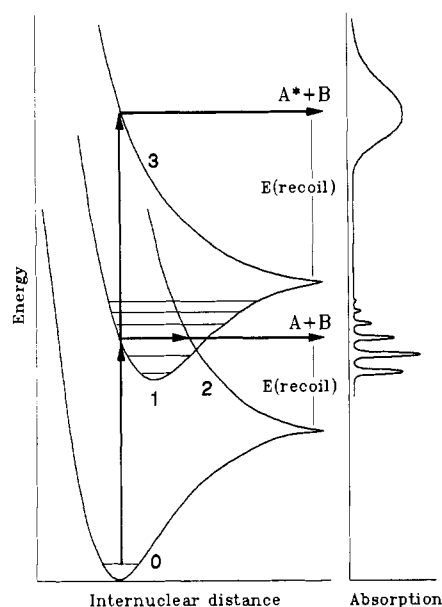
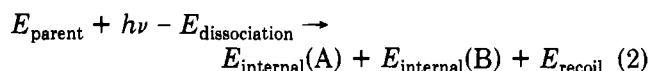


Figure 1. Schematic representation of potential curves and the corresponding absorption spectra for a diatomic molecule. Electronic state 1 is bound, but its levels are predissociated through interaction with the continuum of state 2. The absorption from state 0 to state 1 therefore consists of broadened lines, with widths inversely proportional to the dissociation lifetime. Electronic state 3 is directly dissociative, and the absorption spectrum from state 0 to state 3 consists of a broad continuum.

promoting recoil. But the structures of minimum energy for A and B may change as R_{AB} increases toward dissociation, or the atoms initially connected by the breaking bond may be dynamically coupled to the vibrational modes within A or B. In either case the motion of the atoms during dissociation is not simply one of extension of R_{AB} , and part of the available energy ends up as internal excitation of A and/or B instead of mutual recoil:



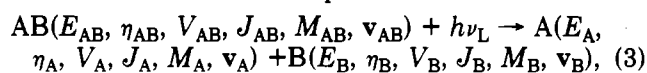
The number of accessible quantum states at a given total energy rises exponentially with the number of modes and, thus, the number of atoms. Energy flow between these modes in large polyatomic molecules is often so fast that their photochemical behavior becomes statistically controlled. Furthermore, in many classes of molecule this leads to the dissipation of the photon energy into heat, thereby diminishing the probability of dissociation. In contrast, dynamical control is the norm in small molecules. This Account is restricted to recent developments involving the latter group of molecules. For these there has been a particularly strong interplay between photochemical and spectroscopic experiments, underpinned by theoretical advances and good quality quantum chemical calculations of molecular potential energy surfaces.

We summarize in section II the experimental advances facilitating a detailed understanding of energy and momentum disposal in photodissociation. Dissociation mechanisms are then discussed in sections III–V, starting with the case of simple recoil.

II. Experimental Techniques

The ideal photochemical experiment, providing the most detailed insight possible into the dynamics of

unimolecular reactions of polyatomic molecules, would completely characterize at a quantum-state-resolved level both the parent molecule and the distribution of motion of its dissociation products:



where E is an internal energy, η is an electronic state, V is a set of vibrational quantum numbers, J and M are a complete set of rotational quantum numbers including spatial quantization, and \mathbf{v} is a translational velocity vector. ν_{L} is the laser frequency. This complete specification, which includes some redundancy through the constraints of conservation laws, has not yet been achieved experimentally.

With highly structured spectra each line may be attributed to a given E , η , V , and J . Thus in favorable cases ν_{L} may be chosen to prescribe the parent state while a tunable laser scans the spectrum of a daughter molecule to determine the distribution over product states through the relative intensities of its spectral lines. Alternatively, ν_{L} can be scanned while the detection frequency is kept fixed, yielding an *action spectrum* for the specific product state. Laser-induced fluorescence (LIF) or multiphoton ionization (MPI) are techniques giving high product sensitivity. Where the spectrum of the parent molecule is unstructured, its quantum state following excitation is less easily specified, since there will usually be a thermal distribution of molecules over the ground-state levels. A common method of avoiding this energy distribution is to use a supersonic jet to cool all the molecules in the sample to the lowest energy level. An alternative that can give a wider choice of initial conditions is to use a two-step excitation: one laser promotes molecules to a selected vibration–rotation level via a well-structured infrared spectrum, and a second laser promotes these selected molecules into a continuum state.

For many years the recoil velocity distribution of photofragments has been measured via times of flight (TOF), using mass spectrometric detection of ions produced by electron bombardment of daughter molecules at the detector end of the flight path,⁴ a very inefficient process. Two recent developments have been to measure the velocities of photofragments via the Doppler shifts of daughter spectral lines⁵ detected by LIF or MPI, or to use laser-based methods to give efficient ionization in the vicinity of the photolysis volume in conjunction with time-of-flight measurements.⁶ These techniques not only enhance sensitivity but also specify the quantum state of the fragments, giving much more information about correlations between the distributions in the internal and recoil motions. Paul Houston has devoted a recent Account to correlated photochemistry based on the use of Doppler shift measurements.⁷

Stereospecific information about the fragmentation process can only be obtained through the correlation of *vector* quantities. The use of polarized laser beams is the key to this aspect.^{8,9} The parent molecule will

(4) Wilson, K. R. In *Excited State Chemistry*; by Pitts, J. N., Ed.; Gordon and Breach: New York, 1970.

(5) Zare, R. N.; Herschbach, D. R. *Proc. IEEE* 1963, 51, 173.

(6) Krautwald, H. J.; Schnieder, L.; Welge, K. H.; Ashfold, M. N. R. *Faraday Discuss. Chem. Soc.* 1986, 82, 163.

(7) Houston, P. L. *Acc. Chem. Res.* 1989, 22, 309.

(8) Greene, C. H.; Zare, R. N. *Annu. Rev. Phys. Chem.* 1982, 33, 119.

have a maximum probability of excitation if its transition dipole (fixed in the molecule) is parallel to the polarized light field (fixed in space). Hence with linear polarization the instantaneous distribution of parent molecules excited from a random sample follows a \cos^2 law in the angle between the directions of the transition dipole μ and the electric field vector ϵ . If there is any stereospecificity in the fragmentation, then the memory of this anisotropy of excitation is carried over into product motion.

For example, the angular distribution of recoil for a given velocity \mathbf{v} of a photofragment generated via a single-photon excitation is most generally expressible as

$$W(\hat{\mathbf{v}}) = \frac{1}{4\pi} [1 + \beta P_2(\hat{\mathbf{v}} \cdot \hat{\boldsymbol{\epsilon}})] \quad (4)$$

$P_2(\cos \theta) = [3 \cos^2(\theta) - 1]/2$ is the second Legendre polynomial, and β is a recoil anisotropy parameter. $\beta = 2$ corresponds to recoil with \mathbf{v} parallel to ϵ , and $\beta = -1$ to perpendicular recoil. β can be determined by measuring the variation of product signal along a fixed flight path as the photolysis polarization vector ϵ is rotated, or by the change in LIF line profile in a Doppler shift experiment as the probe beam direction is changed relative to ϵ . Product rotational motion for a given J state can have a similar anisotropy of distribution in space, usually characterized by the value of an alignment parameter $A_0^{(2)}$ which is the rotational analogue of β but has limits $^{2/5}$ as great (in general $A_0^{(2)}$ lies between $^{4/5}$ for $\mathbf{J} \parallel \mu$ and $^{-2/5}$ for $\mathbf{J} \perp \mu$). Since the transition moment of a molecule rotates with it, we can probe its alignment by using polarized LIF excitation and varying the relative polarizations of photolysis and probe lasers.

III. Direct Dissociation

H₂O. The influence of internal motions in a simple direct dissociation is illustrated by the photochemistry of water vapor in its first electronic absorption band near 165 nm ($\tilde{A}^1B_1 - \tilde{X}^1A_1$).¹⁰ With jet-cooled H₂O at ~ 10 K, the fraction f_r of the available energy that appears as OH rotation is only about 1.2% (i.e., ~ 240 cm⁻¹). This OH rotational excitation could derive from two sources. Even at a low temperature, H₂O molecules have internal motions due to the zero point energy of vibration, and in particular the two H atoms share most of the HOH bending kinetic energy of $\nu_2/4 \sim 415$ cm⁻¹ in the form of relative angular oscillations of the bonds. Upon photolysis ν_2 is a *disappearing vibrational mode* correlating with tangential motion of the H atom and rotation of the OH molecule, thereby imparting an average of ~ 200 cm⁻¹ of rotational energy to the OH. In addition, repulsion between the departing fragments would impart a torque on the OH if the force did not pass through its center of mass, but this appears to be of negligible importance for the \tilde{A} state of H₂O. The two points of note in this system are that (i) the axis of OH rotation is strongly aligned, the sense of which confirms that the rotational motion takes place in the instantaneous plane of the parent H₂O molecule, and (ii) one set of Λ -doublets of the OH radical is much more strongly populated than the other, indicating that

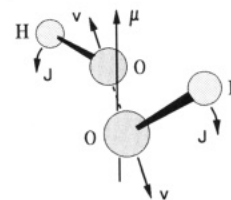


Figure 2. The dynamics of the dissociation of H₂O₂ following excitation in the first absorption band near 250 nm, for which the transition dipole μ bisects the angle between the two OH bonds. The H atoms move toward a trans-planar geometry as the OH radicals start to separate. Thus both the recoil velocities \mathbf{v} and the most probable OH rotational vectors \mathbf{J} are perpendicular to the dipole axis and parallel to each other.

the unpaired electron left behind in OH is strongly constrained to lie in a $2p\pi$ orbital perpendicular to this plane of rotation. This is a clear example of an orbital conservation rule: one electron in water is excited from a $2p\pi$ lone-pair orbital to an in-plane antibonding orbital and goes away on the departing H atom, leaving its unpaired partner behind in the $2p\pi$ orbital of the rotating OH molecule.

Considerably more energy appears as OH vibration ($f_v \sim 10\%$ at 157 nm), with population in $v = 0, 1$, and 2. Dynamical calculations on an ab initio potential surface have shown that in part this excitation has its origin in the symmetry of H₂O. Excitation at the ground-state geometry (a *vertical transition* in accordance with the Franck–Condon principle) leads to a region of the upper-state potential where a repulsion results in an initial symmetric bond stretching. However, there is a high barrier inhibiting dissociation along this coordinate because this would require both bonds to break. A small probability of vibration back to the Franck–Condon region results in slight undulations on the absorption band profile, with a vibrational spacing of ~ 1900 cm⁻¹, but in general the barrier deflects the motion toward stretching of only one bond. Most of the available energy ($f_t \sim 90\%$) is released in simple recoil as this bond breaks and the H and OH move apart, but some of the initial symmetric excitation remains as vibration of the OH bond which did not break.

H₂O₂. Following this simple case it was a surprise to find that the direct dissociation of hydrogen peroxide is strikingly different.^{11,12} Photolysis within the first continuum ($\tilde{A}^1A - \tilde{X}^1A$) at 266 or 248 nm releases about 11% of the available energy into OH rotation but gives no vibrational excitation. However, the novel feature revealed by a polarization study of OH Doppler line profiles is that there is a strong correlation between the fragment rotational and translational vectors \mathbf{J}_{OH} and \mathbf{v}_{OH} , with a clear preference for rotation *around* the axis of recoil. This nontrivial result cannot be the result of initial zero-point energy of disappearing bending vibrations, but is the dynamical consequence of forces that act during the dissociation.

Repulsion between lone-pair electrons on the two O atoms bestows a skewed equilibrium structure on H₂O₂ in its ground state, with a dihedral angle of $\sim 111.5^\circ$ between the OH bonds. The lowest energy electronic transition involves the excitation of one of these lone-pair electrons to an antibonding orbital, as in H₂O. This

(9) Dixon, R. N. *J. Chem. Phys.* **1986**, *85*, 1866.

(10) Andresen, P.; Ondrey, G. S.; Titze, B.; Rothe, E. W. *J. Chem. Phys.* **1984**, *80*, 2548.

(11) Gericke, K. H.; Klee, S.; Comes, F. J.; Dixon, R. N. *J. Chem. Phys.* **1986**, *85*, 4463.

(12) Docker, M. P.; Hodgson, A.; Simons, J. P. *Faraday Discuss. Chem. Soc.* **1986**, *86*, 25.

generates repulsion between the O atoms, promoting HO–OH recoil, but it also removes the twisting force so that the initial motion is for the H atoms to move toward planarity as the fragments move apart. The result of this torque is that the OH radicals recoil in a corkscrew fashion (Figure 2), with much greater rotational excitation than from H₂O. This appears to be a general characteristic of the peroxide bond, and a very similar behavior has been found for the OH fragment from heavier peroxides such as *tert*-butyl hydroperoxide.

IV. Dissociation via Vibrationally Structured Continua

HONO and Alkyl Nitrites. The near-ultraviolet absorption spectra of alkyl nitrites all show diffuse overlapping bands with a mean spacing of about $\nu_2' \simeq 1100 \text{ cm}^{-1}$ characteristic of the vibration of a weak NO bond. The parent acid, HONO, provides a good example of a molecule in which dissociation is slow enough for a partial energy transfer between internal degrees of freedom.^{13,14} Even so, the Doppler widths of the spectra of both the OH and the NO show that about two-thirds of the available energy appears in their mutual recoil.

Dissociation of HONO at 355 nm proceeds via the 2_0^2 band (excitation to the quasi-bound level with $\nu_2' = 2$). This yields OH exclusively in its ground vibrational level, with little rotational excitation ($E_{\text{rot}} \sim 210 \text{ cm}^{-1}$; $f_r \sim 2\%$). In contrast the vibrational levels of NO are populated up to $\nu = 3$ ($f_v \sim 25\%$), each with a high and inverted rotational excitation ($f_r \sim 13\%$). Polarization studies confirm that the rotational motions of both the OH and NO fragments are largely constrained to the original HONO plane. As in the case of H₂O discussed above, the OH rotation derives from disappearing bending modes, of which the in-plane HON vibration has the highest frequency. In contrast, the NO rotation is too energetic for such an origin. The observed Λ -doublet propensities show that an in-plane π -orbital is favored for the unpaired electron of the OH, but an out-of-plane π -orbital for the NO electron. This is consistent with the breaking of the central N–O σ -bond following an out-of-plane $\pi^* \leftarrow n$ excitation within the NO group. The OH line profiles, together with momentum conservation, show that $f_t \sim 60\%$ for the combined recoil energies of OH and NO, so that all the available energy has been accounted for.

The contrasting patterns of OH and NO rotational excitation are readily understood if much of the available energy is released in repulsion directed between the central O and N atoms. A force along this bond passes close to the center of mass of OH, but exerts a strong torque around the more distant center of mass of NO. Thus a significant fraction of this energy release will be channeled into NO rotation, but very little into OH rotation. Model calculations show that the rotational excitation is slightly less than predicted by this simple picture.

The explanation of the vibrational branching has been guided by *ab initio* calculation of the potential energy surface¹⁵ and is illustrated by classical trajec-

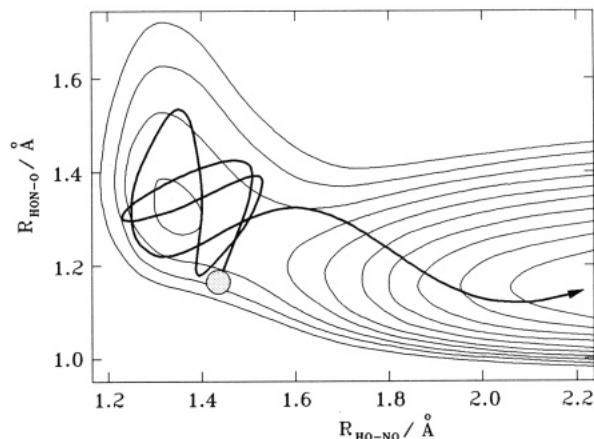


Figure 3. A representative trajectory showing the relative motions in the ON and NO coordinates of HONO following photodissociation at 355 nm in the first absorption band. The initial motion starts in the Franck-Condon region of coordinates (shaded) and is principally a vibration of the terminal NO bond ($\nu_2' = 2$). However, part of the vibrational energy becomes redistributed into motion of the central ON bond, thereby facilitating escape from the shallow potential well and leaving the departing NO in $\nu = 1$.

tories in Figure 3 (note that the complete mechanism involves synchronous oscillation of the ONO angle as well as stretching motions). We can consider this dissociation to occur in two steps. In the first slow step ($\tau \leq 90 \text{ fs}$), V–V transfer partially redistributes the excitation energy between the (HO)N–O and (H)O–N(O) vibrations until the motion is directed toward a well-defined bottleneck. Most of the available energy is then released impulsively in a fast second step during which there is little change in the vibrational distribution of the emerging NO, and the motion is largely confined to a plane thereby generating the translational recoil and NO rotation.

The dissociations of alkyl nitrites follow a similar pattern, albeit with some vibrational excitation of the alkyl radicals. This family therefore typifies Herzberg's predissociation by vibration (case II). The essential feature that gives rise to this behavior is the rapid change in bonding as the central ON bond is stretched. This results in the shallow potential minimum which can support transient vibration, with dissociation driven by the anharmonicity of this potential.

V. Dissociation through Internal Conversion

Many excited states of polyatomic molecules lie at higher energy than possible dissociation products, but have potential energy surfaces that either correlate with excited products of still higher energy or have large potential barriers that hinder vibrational dissociation. Such states might have been expected to be stable against dissociation, and to decay only through fluorescence in the absence of collisions, but this is the exception rather than the rule. The concept of nuclear motion on potential energy surfaces is based on the Born-Oppenheimer approximation that nuclei are infinitely heavier than electrons and, thus, move independently. Even a weak electron–nuclear coupling can promote a rapid radiationless change of electronic state (or *internal conversion*), which may open a path to dissociation on a lower electronic surface. Whereas in

(13) Vasudev, R.; Zare, R. N.; Dixon, R. N. *J. Chem. Phys.* **1984**, *80*, 4863.

(14) Dixon, R. N.; Rieley, H. *J. Chem. Phys.* **1989**, *91*, 2308; *Chem. Phys.* **1989**, *137*, 307.

(15) Suter, H. U.; Huber, J. R. *Chem. Phys. Lett.* **1989**, *155*, 203.

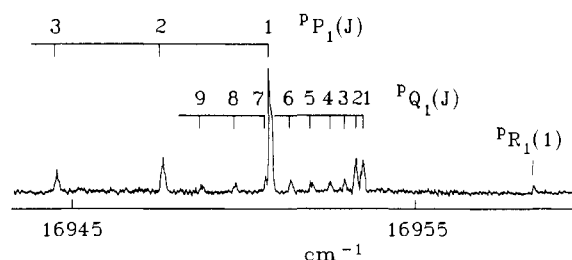


Figure 4. The laser induced fluorescence excitation spectrum of HNO in a band lying above the dissociation threshold to $\text{H} + \text{NO}$. The rapid drop in intensity with increase in J' is a consequence of rotationally induced internal conversion to the continuum of the ground state, followed by dissociation. [$^2P_1(1)$ is the only transition that terminates on $J' = 0$.]

diatomic molecules this predissociation by electronic transition (case I) is mainly restricted to energy levels with classical turning points near curve crossings (Figure 1), such a restriction rarely holds in polyatomic molecules. In general, once such a decay channel is energetically open, the dissociation rate increases with increasing energy. In the Born–Oppenheimer separation the electronic coordinates are referenced to a frame fixed to the nuclei. The coupling then derives from cross-terms in the expression for the total molecular energy which involve products of nuclear momenta and electronic momenta. Where the nuclear momentum arises from vibrational motion, the resultant *vibronic coupling* increases with the vibrational quantum numbers, although some modes may promote internal conversion more effectively than others. *Coriolis coupling* is induced by the angular momentum of molecular rotation and increases with rotational quantum numbers.

The \tilde{A}^1A'' State of XNO Compounds. The LIF excitation spectrum of HNO exhibits a breaking-off in the band structure for all excited levels that lie above $\sim 16450 \text{ cm}^{-1}$, except for a few with $J' = 0$ (Figure 4). Predissociation occurs to $\text{H}(^2S) + \text{NO}(X^2\Pi)$, although direct dissociation on the excited surface is hindered by a substantial potential barrier.¹⁶ In this example the exceptional levels with $J' = 0$ have odd parity to inversion and cannot mix with $J'' = 0$ levels of the ground state which have even parity. Internal conversion is therefore forbidden for such levels. However, for each value of J greater than 0 there are levels of both parities in each state, so that there is no such strict symmetry constraint in the rotating molecule. Dissociation via internal conversion is promoted through the action on the electrons of Coriolis forces generated by the rotation. HCO, H_2O , and NH_3 all have excited states that show similar predissociation through rotationally induced internal conversion.

Larger nitroso compounds such as NCNO or the RNO family have torsional vibrations in which atoms move perpendicularly to the CNO local plane of symmetry. These vibrations play the same role as rotation in HNO in promoting internal conversion from the \tilde{A} to the \tilde{X} state, but for all values of J including 0. Consequently all levels above the dissociation threshold lead to very rapid fragmentation and complete loss of fluorescence.

This mechanism of predissociation by electronic transition involves two steps as with vibrational pre-

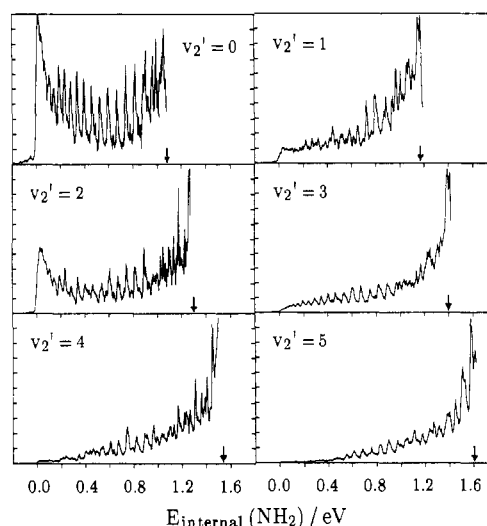


Figure 5. NH_2 internal energy spectra recorded using H-atom time-of-flight spectroscopy following photolysis of jet-cooled NH_3 in its $\tilde{A}-\tilde{X}$ band system. The excitation frequencies are (a) 46200 cm^{-1} (0_0^0 band), (b) 47080 cm^{-1} (2_0^0 band), (c) 47910 cm^{-1} (2_0^2 band), (d) 48872 cm^{-1} (2_0^3 band), (e) 49778 cm^{-1} (2_0^4 band), and (f) 50713 cm^{-1} (2_0^5 band). The vertical arrow by each spectrum is the upper limit set by the available energy [$E(\text{NH}_3) + h\nu - D_0(\text{H}-\text{NH}_2)$].

dissociation but, since the nuclear motion now takes place on two separate potential energy surfaces, there can be great diversity in the ensuing dissociation dynamics.

The \tilde{A}^1A_2'' State of NH_3 . Our final example is the dissociation of ammonia in the 200-nm region. Early attempts to study the energy disposal in the photochemistry of ammonia were frustrated by an inability to assign the spectra of the transient product (presumed to be NH_2), recorded either in emission or by LIF, because of congestion and the ubiquity of unknown spectral lines. The breakthrough came with the development of a method of recording H-atom time-of-flight (TOF) spectra with high resolution and sensitivity.⁶ TOF spectra of the nascent H atoms from monochromatic photolysis of NH_3 (or ND_3) show many sharp peaks, each of which correlates with an internal energy level of the partner NH_2 (or ND_2) (see eq 2).

Whereas ammonia is pyramidal in its ground state, it is planar in its known excited states. Excitation to the zero-point level of the \tilde{A} state near 216 nm gives the simplest TOF spectrum, the intensity being concentrated into a single series of peaks spanning the full range of the available energy of 1.08 eV. Analysis of this spectrum with the aid of a calculated energy level manifold for $\text{NH}_2(\tilde{X}^2B_1)$ reveals that this series corresponds to rotational excitation concentrated about an axis parallel to $\text{H}\cdots\text{H}$ (the a inertial axis).¹⁷ Photolysis at shorter wavelengths proceeds via discrete vibrational levels of NH_3 in which the out-of-plane vibration ν_2' is excited. The trend is for strong population inversion of the NH_2 states as $\nu_2'(\text{NH}_3)$ is increased (Figure 5), accompanied by a lowering of the average recoil energy of both partners. The NH_2 motion remains concentrated in a -axis rotation, but there is also an increasing excitation of the NH_2 bending vibration. However, in addition to this general trend, there is an alternation of internal energy pattern as ν_2' increases from 0 to 3.¹⁸

(16) Dixon, R. N.; Jones, K. B.; Noble, M.; Carter, S. *Mol. Phys.* 1981, 42, 455.

(17) Biesner, J.; Schnieder, L.; Schmeer, J.; Ahlers, G.; Xie, X.; Welge, K. H.; Ashfold, M. N. R.; Dixon, R. N. *J. Chem. Phys.* 1988, 88, 3607.

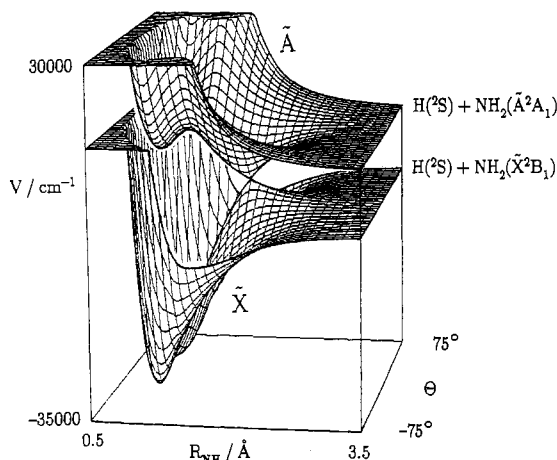


Figure 6. The dependence of the potential energy functions for the \bar{A} and \bar{X} states of NH_3 on one of the dissociation coordinates $R(\text{H}-\text{NH}_2)$ and the out-of-plane angle θ . Within the potential wells θ is proportional to the inversion vibrational coordinate s_2 , whereas when $R \rightarrow \infty$ it becomes the azimuthal angle for rotation of NH_2 about an axis parallel to $\text{H}\cdots\text{H}$ (the a inertial axis). Excitation from the pyramidal ground state of NH_3 to the planar excited state leads to a long progression in ν_2 in the \bar{A} - \bar{X} band system.

The interpretation of these observations has been greatly aided by the results of model dynamical calculations on ab initio potential energy surfaces (Figure 6). These highlight four aspects of the dissociation mechanism. For $\nu_2' = 0$ or 1, dissociation can only proceed by quantum tunneling through a barrier along any one of the NH stretching coordinates, the rates being 1 order of magnitude slower for ND_3 than for NH_3 . A symmetry constraint for nonrotating ammonia requires two quanta of ν_2' for conversion to one quantum of bond stretching, and for $\nu_2' \geq 2$ dissociation is initiated by vibrational redistribution. Thus dissociation from $\nu_2' = 2$ is mediated via anharmonic V-V transfer to the stretching continuum associated with $\nu_2' = 0$, and $\nu_2' = 3$ via $\nu_2' = 1$, as clearly demonstrated by comparisons between the product distributions for $n\nu_2'$ excitation (Figure 5). Vibration-rotation Coriolis coupling between bending and stretching can give an additional rotational enhancement of dissociation mediated via $\Delta\nu_2' = -1$ for which there is some evidence. However, for all values of ν_2' full dissociation to ground-state $\text{H} + \text{NH}_2$ requires a final internal conversion step followed by dissociation on the ground-state surface. The dominant feature of this step is that the \bar{A} and \bar{X} surfaces of NH_3 exhibit a conical intersection in each $\text{N}\cdots\text{H}$ exit channel for planar ammonia (Figure 6). Internal conversion can only proceed by funneling of trajectories originating in nonplanar configurations through these conical intersections, where strong forces amplify the initial inversion motion to generate the high a -axis rotation of the NH_2 product. The final energy disposal is therefore very dependent on the value of $\nu_2'(\text{NH}_3)$ and is strongly influenced by the precise geometry and

(18) Biesner, J.; Schnieder, L.; Ahlers, G.; Xie, X.; Welge, K. H.; Ashfold, M. N. R.; Dixon, R. N. *J. Chem. Phys.* **1989**, *91*, 2901.

forces acting in the vicinity of this transition structure.

The observed polarization dependence of the TOF spectra has revealed a striking aspect of the dissociation dynamics. The majority of departing H atoms follow trajectories lying close to the original plane of the excited molecule. However, where the NH_2 molecule is left in certain very high angular momentum states, the H atom follows a path more nearly perpendicular to this plane.¹⁹ The exact path followed appears to result from a subtle interplay between angular momentum constraints, the heights of centrifugal barriers, and the impact distance at which the H atom breaks free.

The \bar{B}^1A_1 state of H_2O , reached near 130 nm, has many features in common with the \bar{A} state of ammonia.⁶ Again there is a conical intersection in the exit channel of the excited- and ground-state potential energy surfaces, as well as a seam of intersection between the surfaces for the \bar{B}^1A_1 and \bar{A}^1B_1 states which comprise a single $^1\Pi_u$ state for linear H_2O . These surface crossings are associated with strong angular forces which control the dissociation dynamics.

VI. Conclusion

The molecular systems that have been discussed in this Account were chosen to illustrate our qualitative understanding of the factors that control dissociation mechanisms. For a more comprehensive set of reviews of this topic, the reader is referred to a recent book edited by Ashfold and Baggott.²⁰ The most important controlling influences are the topology of the potential energy surface for the initially excited state and of any other states to which internal conversion is feasible, the nature of any non-Born-Oppenheimer coupling between such states, and the relative masses of the atoms in the molecule. The coupling terms are particularly difficult to calculate ab initio, and since surface crossings or degeneracies appear to be ubiquitous along dissociation pathways, there will remain a need to combine innovative theory and experiment to gain new insight into the primary photochemical process. The last 10 years has seen great advances in our experimental ability to probe the detailed dynamics of photodissociation and in the accuracy of theoretical predictions, and doubtless this will continue.

Photodissociation has often been referred to as a *half-collision*, in that the dissociating fragments are initially prepared in contact in a well-characterized manner. A full bimolecular reaction can then be considered as two such half-collisions back to back with a range of close encounters. Although many reactions take place at low total energies on single potential energy surfaces, there is a subset for which surface crossings are important. Their mechanisms will be illuminated by our understanding of photochemical dynamics.

(19) Ashfold, M. N. R.; Dixon, R. N.; Irving, S. J.; Koeppe, H.-M.; Meier, W.; Nightingale, J. R.; Schnieder, L.; Welge, K. H. *Philos. Trans. R. Soc. London, A* **1990**, *332*, 375.

(20) Ashfold, M. N. R.; Baggott, J. E. *Molecular Photodissociation Dynamics*; Royal Society of Chemistry: 1987.